Available online at www.sciencedirect.com
SCIENCE DIRECT®
Biochemical Pharmacology 69 (2005) 1167–1176
Biochemical Pharmacology
www.elsevier.com/locate/biochempharm

Necrotic and apoptotic features of cell death in response to Foscan® photosensitization of HT29 monolayer and multicell spheroids

Sophie Marchal, Anas Fadloun, Estelle Maugain, Marie-Ange D'Hallewin, François Guillemin, Lina Bezdetnaya *

Centre Alexis Vautrin, CRAN CNRS UMR 7039, 54511 Vandoeuvre les Nancy, France

Received 20 August 2004; accepted 24 January 2005

Abstract

Photodynamic therapy (PDT) is an approved anticancer treatment modality that eliminates unwanted cells by the photochemical generation of reactive oxygen species following absorption of visible light by a photosensitizer, which is selectively taken up by tumor cells. Present study reports the modalities of cell death after photosensitization of human adenocarcinoma HT29 monolayer and spheroid cells with a second generation photosensitizer Foscan®. Kinetics of apoptosis and necrosis after Foscan®-PDT in monolayer cells determined by flow cytometry using labeling of cleaved poly(ADP-ribose) polymerase (PARP) and staining with propidium iodide (PI) demonstrated that Foscan® was not a strong inducer of apoptosis and necrosis was a prevailing mode of cell death. Cytochrome *c* release (cyt *c*) and mitochondrial membrane potential ($\Delta\psi_m$) addressed by flow cytometry technique at different time points post-Foscan®-PDT demonstrated that cell photoinactivation was governed by these mitochondrial events. Foscan®-loaded HT29 multicell spheroids, subjected to irradiation with different fluence rates and equivalent light doses, displayed much better tumoricidal activity at the lowest fluence rate used. Apoptosis, measured by caspase-3 activation was evidenced only in spheroids irradiated with the lowest fluence rate and moderate fluence inducing 65% of cell death. Application of higher fluence rates for the same level of photocytotoxicity did not result in caspase-3 activation. The observation of the fluence rate-dependent modulation of caspase-3 activity in spheroids offers the possibility of regulating the mechanism of direct cell photodamage and could be of great potential in the clinical context.

Keywords: Photodynamic therapy; Foscan®; Apoptosis; Mitochondrial events; Caspase-3; Spheroids

1. Introduction

Photodynamic therapy (PDT) is a promising therapeutic strategy for the treatment of superficial, in situ and microinvasive tumors. PDT is based on the administration of tumor-localizing chemicals (photosensitizers) with consecutive non-ionizing illumination of the tumor. PDT induces localized tumor destruction via the photochemical generation of cytotoxic singlet oxygen ($^1O_2$) or other reactive oxygen species. Two principal mechanisms should be considered in PDT-mediated tumor eradication: direct damage of tumor cells and stroma leading to apoptosis and/or necrosis and an indirect pathway, which consist in microvascular injury and non-specific immune activation [1,2].

A second generation photosensitizer Foscan® (meta-tetra(hydroxyphenyl)chlorin (mTHPC)), which displays improved chemical and photophysical properties over Photofrin® (Porfimer sodium), was reported to be mainly localized in the membranes of endoplasmic reticulum (ER) and Golgi [3]. It mediates cell photodamage, principally through singlet oxygen formation [4], and its tumoricidal effect appears to be very sensitive to oxygenation conditions [5,6]. Foscan® has been granted European approval for palliative treatment of patients with

Abbreviations: cyt *c*, cytochrome *c*; ER, endoplasmic reticulum; LD, lethal dose; $\Delta\psi_m$, mitochondrial membrane potential; PARP, poly(ADP-ribose) polymerase; PDT, photodynamic therapy; PI, propidium iodide

* Corresponding author. Tel.: +33 3 83 59 83 06; fax: +33 3 83 59 83 78.
E-mail address: l.bolotine@nancy.fnclcc.fr (L. Bezdetnaya).

0006-2952/$ – see front matter © 2005 Elsevier Inc. All rights reserved.
doi:10.1016/j.bcp.2005.01.021

advanced head and neck cancers who have exhausted all standard treatment options. Recent clinical open-label multicenter studies also reported the efficacy of Foscan®-PDT in the treatment of early squamous cell carcinoma [7,8].

PDT-induced apoptotic response in cultured cells is characterized by the rapid release of mitochondrial cyt *c* into the cytosol with the consecutive cascade of caspases activation, in particular caspase-3, which is a key-element in apoptotic cell death [1,9,10]. PDT-induced apoptosis culminates in chromatin condensation as early as 1–2 h after irradiation [11–15]. Quite frequently, apoptosis and necrosis can be activated simultaneously, the prevailing mechanism of cell death being determined by dosing conditions, cell line, oxygen availability, etc. Therefore, an unfolding and dissection of cell death pathways following photosensitization is worth of interest and should be established for every given photosensitizer.

In many circumstances cells are committed to die before the execution phase of apoptosis starts and this commitment event is coordinated by mitochondria [16,17]. Several studies have suggested the release of mitochondria cyt *c* as a point of no return in photoinduced cell damage [14,16]. Recently, we documented fluence-dependent cyt *c* release immediately after Foscan®-PDT in HT29 cultured cells [18]. A possible approach to elucidate whether cyt *c* release could be a critical lethal event in Foscan®-mediated cell death consists in the detailed post-PDT kinetics of mitochondria alterations.

The ability to manipulate the cell fate machinery is an obvious goal, if a certain type of cell death is required in the clinical context. The rate of light delivery (fluence rate) could be one of the parameters, which allows a modulation of photooxidative substrate damage through the control of tumor oxygenation. The reduction of photodynamic oxygen consumption by using low fluence rates of irradiation clearly improves the Foscan®-PDT treatment outcome in vivo [6,19] and in vitro in multicell tumor spheroids, which serve as an excellent model of small avascular tumors [5]. Similar observations have been reported in spheroids with Photofrin® [20] and ALA-based PDT [21]. Recently, Henderson et al. [22] have shown that the levels of PDT-induced apoptosis using pheophorbide-a derivative were dependent on the fluence rate applied in allografted tumors.

The present study addresses the kinetics of cytochrome *c* release, mitochondrial membrane depolarization and appearance of apoptotic and necrotic cell fractions in HT29 human colon adenocarcinoma cells after Foscan®-PDT with respect to the different levels of cell death. We further assessed apoptosis induction in HT29 tridimensional aggregates by measuring activity of caspase-3. The possibility of fluence rate-dependent modulation of the activity of caspase-3 in spheroids was also investigated.

2. Materials and methods

2.1. Monolayer cell culture

HT29 human adenocarcinoma cells were obtained from ATCC cell collection and regularly controlled for mycoplasma contamination. Cells were maintained in Roswell Park Memorial Institute (RPMI) 1640 medium (Life Technologies) supplemented with 10% heat-inactivated fetal calf serum (FCS) (Costar), 1% penicillin (10,000 IU), streptomycin (10,000 μg/ml) and 1% 200 mM glutamin (Life Technologies). Cells were kept at 37 °C in a 5% CO_2 humidified atmosphere, trypsinized and re-seeded into fresh medium every 7 days. Four days before treatment, 3×10^4 cells/ml were seeded in 60 mm diameter Petri dishes.

2.2. Spheroid cell culture

Multicell spheroids were initiated by seeding 5×10^4 single HT29 cells into 75 cm^2 flasks, previously coated with 1% L-agarose. After 3 days, aggregates were transferred to 250 ml spinner flasks (Integra Biosciences) containing 150 ml of culture medium. The flasks were placed on magnetic plates (Integra Biosciences) at 75 rpm in 5% CO_2 and 37 °C humidified atmosphere. Five days after seeding, aggregates were filtered through 100 and 150 μm sterile nylon screen (VWR International) in order to obtain a homogeneous population of 100–150 μm in diameter. Spheroid culture medium was changed every 2–3 days. When spheroids reached 500 μm in diameter after 15 days culture, they were used for experiments.

2.3. Photosensitizer

Foscan® (mTHPC) was kindly supplied by Biolitec Pharma Ltd. Foscan® stock solution was prepared in methanol. Further dilution was performed in phenol red free RPMI 1640 medium supplemented with 2% fetal calf serum to reach final Foscan® concentrations of 1.45×10^{-6} M and 4.5×10^{-6} M for monolayer and spheroid cultures, respectively.

2.4. Photodynamic treatment of monolayer cells

Logarithmically growing HT29 cells were incubated with 1 μg/ml (1.45×10^{-6} M) Foscan® solution in RPMI supplemented with 2% FCS for 3 h. After two consecutive washings, fresh medium was added and cells were irradiated with a 650 nm laser diode at fluences ranging from 0.06 to 1.92 J cm^{-2} at a fluence rate of 4.5 mW cm^{-2}. Cells were immediately harvested by trypsinization, 4 and 24 h after PDT, for measurements of mitochondrial membrane alterations, apoptotic and necrotic cell number. To assess the effect of the caspase inhibitor zVAD-FMK on

apoptosis and necrosis, a 10^{-2} M stock solution of zVAD-FMK (BD Biosciences) in DMSO was added to cells by dilution 1:500 with cell medium to reach final zVAD-FMK concentration of 2×10^{-5} M. zVAD-FMK solution was added to cells immediately before irradiation and maintained with cells until analysis. Control cells were incubated with Foscan®, with or without zVAD-FMK, and were not subjected to irradiation (drug, no light).

2.5. Photodynamic treatment of spheroid cells

Eighty HT29 spheroids of 500 μm diameter were transferred from the spinner flask to 35 mm Petri dishes. Incubation with 3 ml of complete medium containing 4.5×10^{-6} M of Foscan® was performed at 37 °C, in the dark, for 24 h. After three washes with PBS, spheroids were transferred into 60 mm Petri dishes containing 3 ml culture medium and subjected to irradiation. Irradiations were carried out at 650 nm with a laser diode with various fluences administered at fluence rates of 10, 30 and 90 mW cm^{-2}. The irradiation times were adapted for each fluence rate so that equivalent fluences of 1, 5, 10, 15 and 30 J cm^{-2} were delivered. Control spheroids were exposed to Foscan® and not irradiated (drug, no light).

2.6. Cell survival assays

Cells were collected from the monolayer or from spheroids with trypsin immediately after PDT. They were counted with a Thoma hemocytometer by using trypan blue exclusion assay in order to determine cell yield following PDT treatment. Intact cells were seeded in triplicate into 6-well plates for plating efficiency according to a technique previously described [23]. Briefly, a layer consisting of 1 ml of 0.5% molten agar (Bacto agar, Difco) in culture medium was poured in each well. Over this bottom layer, 10^3 cells were plated in 1 ml culture medium containing 0.3% agar. Cultures were incubated at 37 °C with 5% CO_2 in air for 14 days. Colonies composed of more than 50 cells were counted with an automatic image analysis program (AnalySiS 3.1). The cell yields and the plating efficiencies of each experimental group were normalized to those obtained from control groups (light, no drug), and the overall surviving fraction was determined by computing the product of these two results.

2.7. Apoptosis and necrotic cell fractions assessed by flow cytometry

PARP cleavage is the prominent feature of apoptosis [24]. During apoptosis, PARP is cleaved from its 116 kDa intact form to 85 and 25 kDa fragments. Apoptotic cells were measured by labeling of cleaved PARP with a mouse anti-human monoclonal antibody, which recognizes only the 85 kDa cleaved form of PARP. According to manufacture recommendations (BD Biosciences), 10^5 to 5×10^5 cells were collected after trypsinization, washed with PBS containing 1% FCS and fixed with 250 μl cytofix/cytoperm solution (BD Biosciences) for 20 min at 4 °C. After washing by Perm/Wash solution (BD Biosciences), 0.25 μg monoclonal antibody in 50 μl Perm/Wash solution were added to cells for 30 min at 4 °C. Cells were then washed by Perm/Wash solution and labeled with 5 μl fluorescence isothiocyanate (FITC) conjugated goat anti-mouse polyclonal antibody (DakoCytomation) in 50 μl Perm/Wash solution for 30 min at 4 °C. After washing, cells in 500 μl Perm/Wash solution were analyzed by flow cytometry. The FITC fluorescence ($\lambda_{ex} = 488$ nm, $\lambda_{em} = 519$ nm) was detected in fluorescence channel FL1 with a 530 ± 30 nm band pass filter. Necrotic cells were assessed by flow cytometry after labeling 10^5 cells with 0.03 μM propidium iodide (PI) for 15 min.

2.8. Western blot analysis of PARP

HT29 monolayer cells, treated with light doses of 0.26, 0.64 and 1.92 J cm^{-2}, were collected by scraping 24 h after treatment, washed in ice-cold PBS and treated with lysis buffer, containing 10 mM Tris–HCl (pH 7.4), 1% triton X-100, 1 mM EDTA and 0.1 M phenylmethanesulfonyl fluoride (PMSF) for 30 min on ice and further centrifuged at $15{,}000 \times g$ for 20 min. Protein samples (50 μg) were heated to 95 °C for 7 min in the presence of 5% 2-mercaptoethanol, chilled on ice and subjected to SDS–PAGE analysis, followed by electrophoretic transfer to polyvinylidene difluoride (PVDF) membranes. Membranes were blocked with 5% non-fat dry milk in PBS and 0.5% Tween-20 for 1 h at room temperature and afterwards were incubated overnight at 4 °C with purified mouse anti-cleaved PARP (Asp 214) monoclonal antibody (1:2000). After several washes the blots were incubated with secondary anti-mouse IgG linked to horseradish peroxidase (1:1000). The antigens were detected using the ECL detection system (Amersham Biosciences) and visualized by autoradiography.

2.9. Measurements of the mitochondrial membrane depolarization

The green fluorescent probe 5,5′,6,6′-tetrachloro-1,1′,3,3′-tetraethylbenzimidazolylcarbocyanine iodide, JC-1 (Molecular Probes) exists as a monomer at low membrane potential and at higher potentials, JC-1 forms red fluorescent aggregates. The use of this probe in the measurement of $\Delta\psi_m$ after PDT has been described previously [25]. Trypsinized cells (5×10^5 cells) were centrifuged at $400 \times g$. Cell pellet was suspended in 1 ml medium containing 1 μl of JC-1 (final concentration 5 μg/ml). After a 15 min incubation at 37 °C, cell suspension was measured by flow cytometry (FACSCalibur). The aggregate fluorescence ($\lambda_{ex} = 488$ nm,

λ_{em} = 590 nm), detected in fluorescence channel FL2 with a 585 ± 42 nm band pass filter can easily be separated from the monomer fluorescence (λ_{ex} = 488 nm, λ_{em} = 527 nm) detected in fluorescence channel FL1 with a 530 ± 30 nm band pass filter.

2.10. Measurements of cytochrome c release

Cytochrome *c* release was estimated by labeling digitonin-permeabilized cells with APO2.7 phycoerythrin (PE)-conjugated monoclonal antibody (Beckman Coulter) [26]. Trypsinized (0.5–1) × 10^6 cells were permeabilized with 0.1 μg/ml digitonin for 20 min at 4 °C, washed and labeled with PE-APO2.7 (dilution 1/5) for 15 min at room temperature. After washing, cells were measured by flow cytometry using excitation at 488 nm and fluorescence emission at 585 ± 42 nm (FL2).

2.11. Quantification of caspase-3 activity in spheroids

For each experimental point, cells obtained from 80 spheroids and 24 h after treatment were washed with PBS, and the pellet obtained after centrifugation was stored at −20 °C until use. Spheroids were dissociated in 1 ml lysis buffer composed with 10% sucrose, 20 mM Hepes, 0.1% chaps, 2 mM dithiotreitol, 1 mM EDTA, 1 μg/ml pepstatin, 1 μg/ml leupeptin and 100 μg/ml phenylmethylsulfonyl fluoride (PMSF), pH 7.4. The cell lysate was incubated on ice for 30 min, sonicated twice for 10 s and centrifugated (10 min, 10,000 × *g*). 800 μl of supernatant were incubated with 200 μl (6 × 10^{-6} M) highly specific caspase-3 fluorogenic substrate DEVD-AFC (Asp-Glu-Val-Asp, DEVD conjugated with 7-amino-4-trifluoromethylcoumarin, AFC) (BD Biosciences) in lysis buffer at 37 °C for 1 h. The specificity of caspase-3 activity was verified by adding 0.05 × 10^{-6} M DEVD-CHO for 2 h. In all cases, a complete inhibition of the enzymatic reaction was obtained. The released fluorescent product was measured spectofluorimetrically ($\lambda_{ex/em}$ 400 nm/450–550 nm; Perkin-Elmer L2259051). The raw data were normalized per mg protein. Protein concentrations were estimated in cell lysates by using the Bio-Rad assay. The final results were expressed as the ratio between the experimental and the control normalized values.

2.12. Imaging of Foscan® distribution in HT29 spheroids

Spheroids incubated with 4.5 × 10^{-6} M of Foscan® during 24 h in the dark were placed in a freezing medium (Jung, Leica), frozen at −25 °C and sectioned into 6 μm microscope slides using a cryostat (Leica CM1850). Preparations were mounted with an aqueous medium (Menzel superfrost color). Spheroid sections were then observed under a fluorescence microscope (Leica DMRB). Excitation filter: band pass 450–490 nm.

2.13. Statistical analysis

Mann–Whitney's *U* test was employed to determine the statistical significance with a limit set to $p < 0.05$ using Staview 5.0 software.

3. Results

3.1. Cell viability in HT29 monolayer cultured cells photosensitized with Foscan®

Loss of cell viability of HT29 cells subjected to Foscan®-based PDT was assessed by clonogenic assay after irradiation with a range of light fluences (Fig. 1). Fluences of 0.26, 0. 64 and 1.92 J cm^{-2} were chosen for further examination of mitochondrial alterations and modalities of cell death. The corresponding loss of viability was 60, 91 and 97%.

3.2. Apoptotic and necrotic cell death after photosensitization with Foscan®

Modalities of cell death imposed on HT29 cells by Foscan®-PDT were approached by flow cytometry quantification of apoptotic and necrotic cells. Number of apoptotic cells was deduced from the specific labeling of 85 kDa fragment of cleaved PARP. PARP cleavage was confirmed by immunoblotting at 24 h post-PDT. Necrotic cells were measured with a high-affinity nucleic acid probe PI that easily penetrates cells with compromised plasma membranes and does not cross the membranes of living cells.

Fig. 2a and b presents the evolution of apoptotic response at different post-PDT intervals in HT29 cells subjected to LD_{97}. Shortly after PDT (4 h), the percentage of fluorescent cells significantly augmented in M1 gate

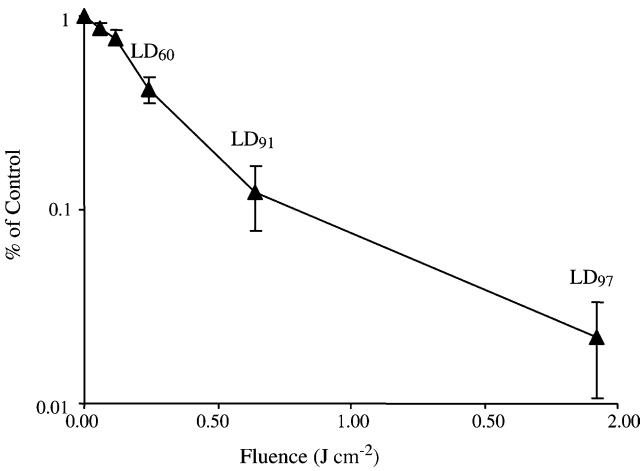

Fig. 1. Dose dependence of cell killing in HT29 cells sensitized with Foscan® (1.45 × 10^{-6} M, 3 h). The percentage of cell survival was counted by clonogenic assay15 days after PDT. Results are the mean ± S.E.M. of at least three independent experiments.

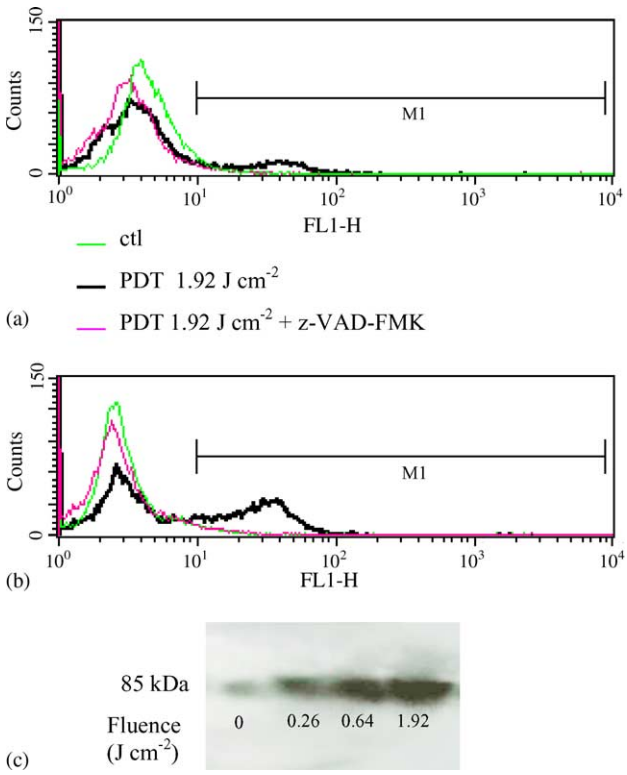

Fig. 2. The effect of Foscan® photosensitization on PARP cleavage in HT29 cells assessed by flow cytometry (a, b) and by Western blotting (c). (a, b) Cells were exposed to 1.45×10^{-6} M Foscan® for 3 h, irradiated at 1.92 J cm^2 (LD_{97}) with red light ($\lambda = 652$ nm), labeled with anti-cleaved PARP mouse monoclonal antibody and a FITC-labeled secondary anti-mouse antibody. Histograms of log scale green FITC fluorescence (*x*-axis, FL1-H) as a function of cell counts (a) 4 h and (b) 24 h after PDT. (c) Cells were exposed to 1.45×10^{-6} Foscan® for 3 h, irradiated at 0.26, 0.64 and 1.92 J cm^{-2} with red light ($\lambda = 652$ nm) and 24 h later analyzed by Western blotting with monoclonal mouse antibody to cleaved PARP.

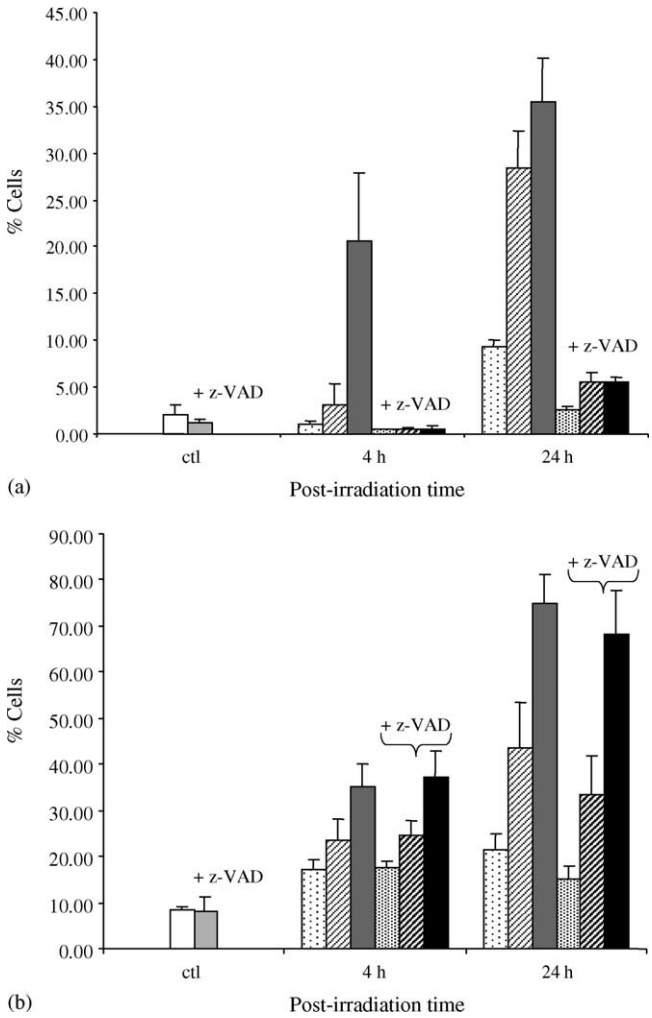

Fig. 3. Kinetics of post-PDT accumulation of apoptotic (a) and necrotic (b) HT29 cells in response to sensitization with Foscan® (1.45×10^{-6} M, 3 h). Cells were irradiated at 0.26 J cm^{-2} in the absence (⬚) or in the presence (▨) of z-VAD-FMK; at 0.64 J cm^{-2} in the absence (▨) or in the presence (▨) of z-VAD-FMK and at 1.92 J cm^{-2} in the absence (■) or in the presence (■) of z-VAD-FMK. Control cells (light, no drug) without (□) or with (▩) z-VAD-FMK. Results are the mean of at least three independent experiments.

compared to control cells (drug, no light) (Fig. 2a). At 24 h post-PDT about 35% cells underwent PARP cleavage (Fig. 2b). Apoptosis was inhibited to the level of untreated cells when irradiation was performed in the presence of caspase inhibitor z-VAD-FMK (Fig. 2a and b).

PARP cleavage at 24 h after irradiation at three light doses was further confirmed by Western blotting (Fig. 2c). With the increase in the light doses, a progressive increase in the expression level of 85 kDa cleaved band was detected.

Fig. 3 displays the kinetics of accumulation of apoptotic and necrotic cells with and without z-VAD-FMK with respect to the applied fluences. A sharp increase in the number of apoptotic cells was observed at 4 h post-PDT with the highest fluence, while two lower fluences did not differ significantly from control values (Fig. 3a). A maximum of apoptotic cells ($35.4 \pm 6.8\%$) was registered 24 h post-PDT with the highest fluence, and this value was not significantly different ($p = 0.27$) from that at the fluence of LD_{91} ($28.4 \pm 5.6\%$). A slight but still statistically significant increase in apoptosis over control treatment was registered 24 h post-PDT for cells irradiated with LD_{60}. Decrease in apoptotic cells to the levels of untreated controls was registered in the presence of z-VAD-FMK at all applied fluences and both post-PDT time points (Fig. 3a).

Necrosis augmented with time post-PDT and increasing light doses (Fig. 3b). Irradiation with high light fluences (LD_{91} and LD_{97}) resulted in a steady increase in necrotic fractions with time after treatment with an accumulation of, respectively, $43.60 \pm 16.8\%$ and $74.9 \pm 11.0\%$ PI positive cells at 24 h post-PDT. Cells subjected to irradiation with the lowest dose (LD_{60}) exhibited different kinetic profile with a slow increase in necrotic cell fraction reaching $21.6 \pm 5.6\%$ at 24 h after treatment (Fig. 3b). Presence of z-VAD-FMK during and after irradiation did not significantly affect PDT-mediated necrosis, irrespective of light fluences and times post-PDT.

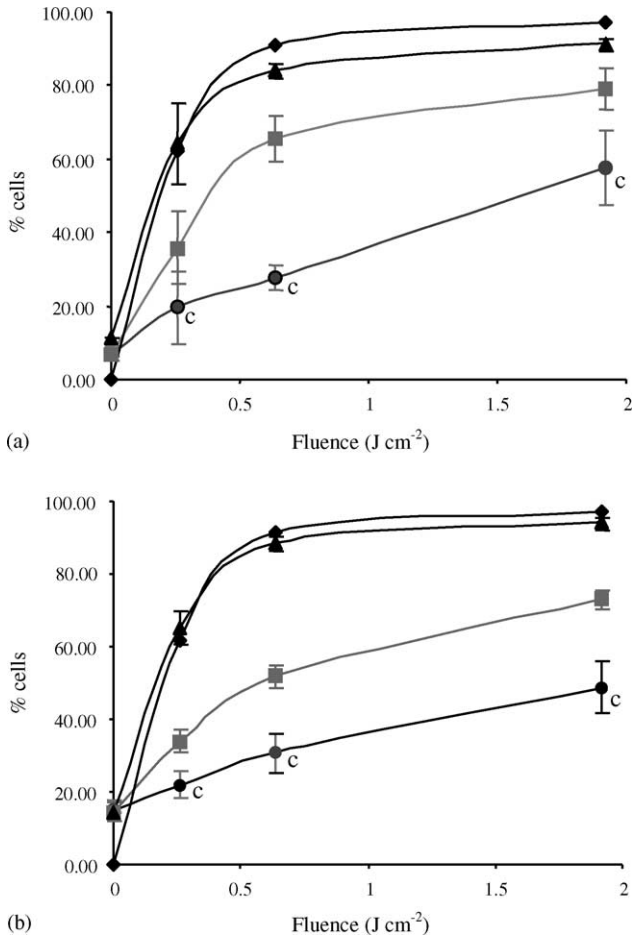

Fig. 4. Fluence-related (a) cytochrome *c* release and (b) mitochondrial membrane depolarization in Foscan®-photosensitized HT29 adherent cells. Data on the loss of clonogenicity (◆) are taken from Fig. 1. Cells were analyzed 4 h (■) and 24 h (▲) after irradiation. The letter 'c' indicates data from Marchal et al. [18]. Results are the mean ± S.E.M. of at least three independent experiments.

3.3. Photoinduced cytochrome c release and mitochondrial membrane depolarization in monolayer HT29 cells

The fluence-dependent cyt *c* release and alterations of $\Delta\psi_m$ at 4 and 24 h after Foscan® photosensitization are displayed in Fig. 4a and b and our previous data on mitochondrial membrane damage, tested immediately after PDT [18] are included for comparison. In contrast to the loss of mitochondrial membrane functions immediately after PDT, at 4 h post-PDT the profile of cyt *c* release paralleled that of the loss of cell viability with a noticeable similarity 24 h post-PDT (Fig. 4a). At this time point, the percentage of cells with cyt *c* release matched perfectly the percentage of dead cells observed at every applied fluence (64, 84 and 92% versus 60, 91 and 97%).

The loss of $\Delta\psi_m$ demonstrated the same kinetic pattern as that of cyt *c* release (Fig. 4b), except for a slight difference at 4 h post-PDT, thus suggesting that both photoinduced cyt *c* release and mitochondrial membrane depolarization are concomitant and correlated events.

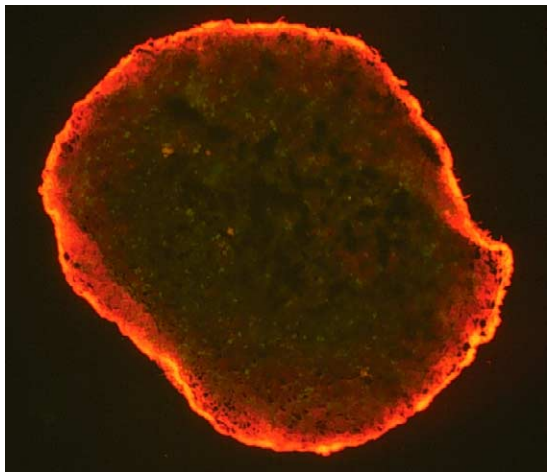

Fig. 5. Fluorescence photomicrograph of a typical 6 μm thick frozen section from the Foscan®-sensitized HT29 spheroid of 500 μm in diameter.

3.4. Foscan® distribution in HT29 multicell tumor spheroids

The Foscan® distribution in spheroid is presented in Fig. 5. A strong pattern of the dye fluorescence, observed in the outer rim of the spheroid, falls off quickly from the spheroid surface and represents a weak constant fluorescence in the spheroid center.

3.5. Effects of fluence rates of irradiation on Foscan®-photosensitized HT29 spheroids

Foscan®-loaded spheroids were irradiated with a range of light fluences delivered at three different fluence rates of 10, 30 and 90 mW cm^{-2}. As the fluence rate was reduced from 90 to 10 mW cm^{-2}, the overall survival was dramatically diminished for equivalent doses of light (Fig. 6). For example, for the fluence of 10 J cm^{-2}, the percentage of viable cells was 71, 49 and 4% in response to the fluence rates of 90, 30 and 10 mW cm^{-2}.

3.6. Evaluation of caspase-3 activation in HT29 spheroids

Caspase-3 activation after photodynamic treatment of spheroids was employed as a measure of apoptosis. Table 1 presents the results of caspase-3 activation and photocytotoxicity after illumination with the fluence rate of 10 mW cm^{-2} at three different fluences (1, 5 and 10 J cm^{-2}) corresponding to LD_{17}, LD_{65} and LD_{96}. At LD_{17} and LD_{96} caspase-3 activity was not significantly different from control cells. In contrast, caspase-3 activation at LD_{65} was 2.6-fold above the level of untreated cells ($p = 0.021$).

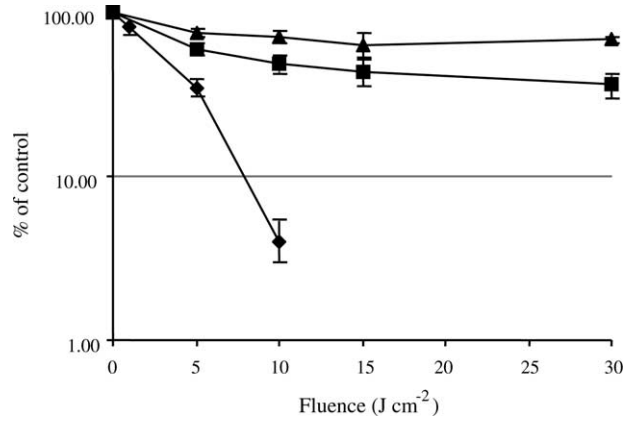

Fig. 6. Dose dependence of overall survival of cells dissociated from Foscan®-sensitized HT29 spheroids (4.5×10^{-6} M, 24 h) treated with PDT delivered at fluence rates of 10 mW cm^{-2} (◆), 30 mW cm^{-2} (■) or 90 mW cm^{-2} (▲). The percentage of cell survival was counted by clonogenic assay 15 days after PDT. Results are the mean ± S.E.M. of at least three independent experiments.

Table 1
Caspase-3 induction 24 h post-PDT in Foscan®-sensitized HT29 spheroids (4.5×10^{-6} M, 24 h) irradiated at the fluence rate of 10 mW cm^{-2} with different light fluences

Fluence (J cm^{-2})	Photocytotoxicity % of control	Caspase-3 fold induction	Statistics (p)
1	17	1.40 ± 0.89	0.25
5	65	2.62 ± 1.07	0.021*
10	96	1.42 ± 0.36	0.064

* Statistically significant value given by the Mann–Whitney's U test ($p < 0.05$).

We further compared the induction of apoptosis in spheroids treated with three fluence rates and light doses inducing a photocytotoxicity of 65%. Caspase-3 activation at 30 and 90 mW cm^{-2} was, respectively, 1.17 ± 0.06 and 1.12 ± 0.24 fold induction and did not significantly differ from the control values. Thus, among all fluence rates used, only the fluence rate of 10 mW cm^{-2} resulted in a significant caspase-3 induction for a given level of photocytotoxicity of 65%.

4. Discussion

The modalities of cell death provided by photodynamic treatment are still under investigation and the complexity of a network of survival and death pathways has been recently reviewed by Agostinis et al. [27].

Apoptosis has been found to be a prominent form of cell death in many cells after photosensitization. The pathways in which apoptotic cells are engaged after PDT, the intensity and the rapidity of the process are mainly dependent on the cell line, the subcellular localization of the photosensitizer and the extent of photooxidative damage [1,2,28–30].

We have chosen to follow apoptosis in Foscan®-photosensitized HT29 cells. The number of necrotic and apoptotic cells (Fig. 3a and b) displayed a significant increase with increasing time and light dose. However, the general pattern of necrotic and apoptotic cells' distribution was in favor of necrosis. In particularly, at 24 h post-PDT the number of necrotic cells (Fig. 3b) displayed a dramatic increase with increasing light dose (21 ± 6%, 44 ± 17% and 75 ± 11% at LD_{60}, LD_{91} and LD_{97}, respectively), while the number of apoptotic cells increased from 9 ± 1% to 28 ± 6% with no further increase at the highest fluence applied (28 ± 6% versus 35 ± 7%, $p = 0.27$).

The presence of a broad spectrum caspase inhibitor (z-VAD-FMK) during and after irradiation completely abrogated Foscan®-PDT apoptosis upon all treatment conditions (Fig. 3a). At the same time, no significant difference was observed for necrosis (Fig. 3b). Together with our previous observation on caspase-3 activation in HT29 cells subjected to Foscan®-PDT [18], the present one points out to caspase-dependent nature of apoptotic process mediated by Foscan® photosensitization. Further, the lack of inhibitory effect of z-VAD-FMK on necrotic cells presumes that necrosis is directly induced by photodamage rather than being secondary to apoptosis.

Taken as a whole, the mild level of post-PDT apoptosis observed in the present study is likely to be related to the specificity of Foscan® localization. The preferential Foscan® localization in the Golgi/reticulum complex was microscopically observed in human and murine mammary malignant cells [3,31]. In all likelihood this localization pattern could be extended to HT29 cells, as can be deduced from primarily photodamaged Golgi apparatus after Foscan®-PDT in HT29 cultured cells [32]. Thus, the Golgi/reticulum complex could be a site from which the cell death signals originate and converge on mitochondria to trigger the apoptotic process in a less efficient manner than mitochondria-targeting photosensitizers. Similar observation was reported for other reticulum/Golgi localizing photosensitizers [29,33].

Mitochondria play a key role in the pathways of cell death either by mitochondrial proteins involved in the apoptotic process or by the loss of functionality resulting in ATP depletion [34]. It has been suggested that in response to different stimuli, including photooxidative stress, the cell may be irreversibly committed to death once mitochondrial cyt c is released into the cytosol [16,17,35,36]. The proposal on the critical role of cyt c in the PDT damage was based on the observation that photoinduced release of cyt c proceeds normally in cells irrespective of the functional activity of caspases [16]. Another argument was the good correlation in dose–response between the fraction of cells that release cyt c shortly (30 min) after PDT with mitochondria localized photosensitizer phtalocyanine (Pc) 4 and overall survival [14]. Considering ER/Golgi localization of Foscan®, a certain delay was anticipated for the complete release of

cyt *c* from photokilled cells. Therefore, we studied a detailed post-PDT kinetics of mitochondrial alterations (Fig. 4a and b). Although immediately after irradiation, the kinetic of the loss of mitochondrial membrane functions was very different from that of cell viability, the situation changed from 4 h post-PDT. This early time point evidenced a very good correlation between mitochondrial membrane damage and cell photokilling at each PDT dose. Twenty-four hours post-Foscan®-PDT, the percentage of cells undergoing $\Delta\psi_m$ dissipation and cyt *c* release matched perfectly the percentage of dead cells. This kinetic study clearly shows that both apoptotic and necrotic pathways implicated in Foscan®-mediated HT29 cell photoinactivation are governed by mitochondrial membrane photodamage, thus suggesting the cyt *c* release and mitochondrial membrane depolarization as the critical lethal events for Foscan® photosensitization. However, we cannot discard the possibility that the lethal event, which commits the cells to death lie upstream mitochondria. Such possibility was proposed in the recent study of Chiu et al. [37], where the authors reported the same level of Pc-4 photocytotoxicity whether or not cyt *c* was released after irradiation. Considering a high affinity of Foscan® for ER/Golgi complex, the effects of Foscan®-PDT on the ER proteins, which could be critical for cell death, deserve further investigation.

Another observation from the plots displayed on Fig. 4 is that the both cyt *c* release and $\Delta\psi_m$ dissipation are concomitant events. Contradictory results have been obtained regarding the timing of these both mitochondrial events. Photoinduced cyt *c* release from the mitochondrial intermembrane space to the cytosol simultaneously with the loss of $\Delta\psi_m$ was reported for porphycenes in leukemia cells and for mTHPC in adherent and myeloid cells [11,15,35]. In contrast, other studies separated the dissipation of $\Delta\psi_m$ and cyt *c* release, as has been demonstrated for Pc-4, Hypericin- and chlorin-type photosensitizer [25,38,39].

The comprehension of cell death mechanisms in vivo is always a challenge, since apoptotic/necrotic events can arise from the vascular tumor network as well as from direct photodamage of tumor cells. In this context, the three-dimensional arrangements of tumor cells in spheroids provides biochemical and histological similarities to small avascular tumors in vivo and allows the specific study of direct photocytotoxic effects of PDT.

The efficacy of Foscan®-based PDT has been related to the maintenance of tumor oxygenation. As illustrated in Fig. 6, therapeutic efficacy increased progressively when the fluence rate was reduced over the range of 90 to 10 mW cm^{-2}. Even high light doses delivered at fluence rates of 90 and 30 mW cm^{-2} were unable to produce more than 60% cell death. This loss in efficacy could be attributed to a protective effect from Foscan®-mediated photochemical reaction in spheroids due to the photochemical oxygen depletion at high fluence rates. Conversely, an enhanced photocytotoxic effect observed at 10 mW cm^{-2} could be explained by the extension of the singlet oxygen dose into the central regions of the spheroid [5]. Following these observations, we evaluated apoptosis by measuring caspase-3 activity in Foscan®-photosensitized spheroids at different levels of cell death and at the efficient fluence rate of 10 mW cm^{-2}. Among all fluences tested, only at the light dose inducing 65% cell death, we observed statistically significant activation of caspase-3 (2.62-fold induction, $p = 0.021$) (Table 1). Adherent HT29 cells subjected to the same level of photodamage (LD_{60}) were characterized by a 12-fold increase in caspase-3 activation 24 h after Foscan® photosensitization [18]. The considerably lower level of caspase-3 induction in HT29 three-dimensional arrangements contrary to monolayer cells could be related to the fact that cells at the core or the periphery of the spheroid do not receive the same dose of photosensitizer and oxygen. Indeed, Foscan® fluorescence distribution in spheroid sections (Fig. 5) demonstrated a non-uniform sensitizer penetration with an intense Foscan® fluorescence in the outermost rim of the spheroid and a considerably reduced dye fluorescence inside the spheroid. Consequently, the response of cells to photosensitization is inhomogeneous with the external cells being the most photosensitive.

An important observation from the spheroid study is that application of higher fluence rates of 30 and 90 mW cm^{-2} for the same level of photocytotoxicity of LD_{65} did not result in caspase-3 activation. This observation offers the possibility of modulating the mechanism of direct cell photodamage and could be helpful in designing future clinical protocols. Oxygen-conserving low fluence rate protocols favoring apoptosis should be recommended when PDT is applied for the curative treatment of in situ neoplasia or/and as a palliative de-obstructing treatment modality. In both cases, a rapid shrinking of the tumor mass is expected and apoptosis without accompanying inflammatory reaction and swelling should be favored above complete tumor eradication. On the other hand, when the goal of PDT is to cure an infiltrative tumor that is possibly already micro-spreading beyond the margins of the illumination spot, necrosis with its accompanying inflammatory reaction may be recommended. However, the protocols employing high fluence rates should be finely tuned, since oxygen-depleting regimens may significantly limit treatment outcome.

In conclusion, we have demonstrated a mild apoptotic response following HT29 monolayer cells photosensitization with Foscan® together with a significant increase in necrosis with increasing time and light dose. Both apoptotic and necrotic pathway implicated in Foscan®-mediated HT29 cell photoinactivation are governed by mitochondrial membrane photodamage manifested by cyt *c* release and $\Delta\psi_m$ dissipation. HT29 spheroids treated with Foscan®-PDT at different fluence rates and equivalent light doses evidenced apoptotic induction only at moderate

fluence rate and fluence inducing 65% cell killing. Application of higher fluence rate did not result in caspase-3 activation. Fluence rate modulation of apoptosis in spheroids could contribute to the optimization of clinical protocol.

Acknowledgments

This work was supported by Alexis Vautrin Cancer Center Research Funds, French Ligue Nationale contre le Cancer. We gratefully acknowledge Biolitec Pharma Ltd. for providing the Foscan®.

References

[1] Oleinick N, Morris RL, Belichenko I. The role of apoptosis in response to photodynamic therapy: what, where, why, and how. Photochem Photobiol Sci 2002;1:1–21.
[2] Dougherty TJ, Gomer CJ, Henderson BW, Jori G, Kessel D, Korbelik M, et al. Photodynamic therapy. J Natl Cancer Inst 1998;90:889–905.
[3] Teiten MH, Bezdetnaya L, Morlière P, Santus R, Guillemin F. Endoplasmic reticulum and Golgi apparatus are the preferential sites of Foscan® localization in cultured tumor cells. Br J Cancer 2003;88:146–52.
[4] Melnikova VO, Bezdetnaya LN, Potapenko AY, Guillemin F. Photodynamic properties of meta-tetra(hydroxyphenyl)chlorin in human tumor cells. Radiat Res 1999;152:428–35.
[5] Coutier S, Mitra S, Bezdetnaya L, Parache RM, Georgakoudi I, Foster TH, et al. Effects of fluence rate on cell survival and photobleaching in meta-tetra-(hydroxyphenyl)chlorin-photosensitized Colo 26 multicell tumor spheroids. Photochem Photobiol 2001;73:297–303.
[6] Coutier S, Bezdetnaya LN, Guillemin F, Parache RM, Foster TH. Effect of irradiation fluence rate on the efficacy of photodynamic therapy and tumor oxygenation in meta-tetra(hydroxyphenyl)chlorin (MTHPC)-sensitized HT29 xenografts in nude mice. Radiat Res 2002;158:339–45.
[7] Hopper C, Niziol C, Sidhu M. The cost-effectiveness of Foscan mediated photodynamic therapy (Foscan-PDT) compared with extensive palliative surgery and palliative chemotherapy for patients with advanced head and neck cancer in the UK. Oral Oncol 2004;40:372–82.
[8] D'Cruz A, Robinson MH, Biel MA. mTHPC-mediated photodynamic therapy in patients with advanced, incurable head and neck cancer: a multicenter study of 128 patients. Head Neck 2004;26:232–40.
[9] Varnes ME, Chiu SM, Xue LY, Oleinick NL. Photodynamic therapy-induced apoptosis in lymphoma cells: translocation of cytochrome *c* causes inhibition of respiration as well as caspase activation. Biochem Biophys Res Commun 1999;255:673–9.
[10] Cohen GM. Caspases: the executioners of apoptosis. Biochem J 1997;326:1–16.
[11] Kessel D, Luo Y. Photodynamic therapy: a mitochondrial inducer of apoptosis. Cell Death Differ 1999;6:28–35.
[12] He J, Whitacre CM, Xue LY, Berger NA, Oleinick NL. Protease activation and cleavage of poly(ADP-ribose) polymerase: an integral part of apoptosis in response to photodynamic treatment. Cancer Res 1998;58:940–6.
[13] Granville DJ, Jiang H, An MT, Levy JG, McManus BC, Hunt DWC. Overexpression of Bcl-x_L prevents caspase-3-mediated activation of DNA fragmentation factor (DFF) produced by treatment with photochemotherapeutic agent BPD-MA. FEBS Lett 1998;422:151–4.
[14] Chiu S, Evans HH, Lam M, Nieminen A, Oleinick NL. Phthalocyanine 4 photodynamic therapy-induced apoptosis of mouse L5178Y-R cells results from a delayed but extensive release of cytochrome *c* from mitochondria. Cancer Lett 2001;165:51–8.
[15] Chen JY, Mak NK, Yow CM, Fung MC, Chiu LC, Leung WN, et al. The binding characteristics and intracellular localization of temoporfin (mTHPC) in myeloid leukemia cells: phototoxicity and mitochondrial damage. Photochem Photobiol 2000;72:541–7.
[16] Xue LY, Chiu SM, Oleinick NL. Photodynamic therapy-induced death of MCF-7 human breast cancer cells: a role for caspase-3 in the late steps of apoptosis but not for the critical lethal event. Exp Cell Res 2001;263:145–55.
[17] Green DR, Reed JC. Mitochondria and apoptosis. Science 1998;281:1309–12.
[18] Marchal S, Bezdetnaya L, Guillemin F. Modality of cell death induced by Foscan®-based photodynamic treatment in human colon adenocarcinoma cell line HT29. Biochemistry (Mosc) 2004;69:45–9.
[19] Van Geel IP, Oppelaar H, Marijnissen JP, Stewart FA. Influence of fractionation and fluence rate in photodynamic therapy with Photofrin or mTHPC. Radiat Res 1996;145:602–9.
[20] Foster TH, Hartley DF, Nichols MG, Hilf R. Fluence rate effects in photodynamic of multicell tumor spheroids. Cancer Res 1993;53:1249–54.
[21] Madsen SJ, Sun CH, Tromberg BJ, Wallace VP, Hirschberg H. Photodynamic therapy of human glioma spheroids using 5-aminolevulinic acid. Photochem Photobiol 2000;67:612–25.
[22] Henderson BW, Gollnick SO, Snyder JW, Busch TM, Kousis PC, Cheney RT, et al. Choice of oxygen-conserving treatment regimen determines inflammatory response and outcome of photodynamic therapy of tumors. Cancer Res 2004;64:2120–6.
[23] Merlin JL, Azzi S, Lignon D, Ramacci C, Zeghari N, Guillemin F. MTT assays allow quick and reliable measurement of the response of human tumour cells to photodynamic therapy. Eur J Cancer 1992;28A:1452–8.
[24] Patel T, Gores GJ, Kaufmann SH. The role of proteases during apoptosis. FASEB 1996;10:587–97.
[25] Chiu SM, Oleinick NL. Dissociation of mitochondrial depolarization from cytochrome *c* release during apoptosis induced by photodynamic therapy. Br J Cancer 2001;84:1099–106.
[26] Carthy CM, Granville DJ, Jiang H, Levy JG, Rudin CM, Thompson CB, et al. Early release of mitochondrial cytochrome *c* and expression of mitochondrial epitope 7A6 with prophyrin-derived photosensitizer: Bcl-2 and Bcl-x_L overexpression do not prevent early mitochondrial events but still depress caspase activity. Lab Invest 1999;79:953–65.
[27] Agostinis P, Buytaert E, Breyssens H, Hendrickx N. Regulatory pathways in photodynamic therapy induced apoptosis. Photochem Photobiol Sci 2004.
[28] Vantieghem A, Assefa Z, Vandenabeele P, Declercq W, Courtois S, Vandenheede JR, et al. Hypericin-induced photosensitization of HeLa cells leads to apoptosis or necrosis. Involvement of cytochrome *c* and procaspase-3 activation in the mechanism of apoptosis. FEBS Lett 1998;440:19–24.
[29] Piette J, Volanti C, Vantieghem A, Matroule JY, Habraken Y, Agostinis P. Cell death and growth arrest in response to photodynamic therapy with membrane-bound photosensitizers. Biochem Pharmacol 2003;66:1651–9.
[30] Dellinger M. Apoptosis or necrosis following Photofrin photosensitization: influence of the incubation protocol. Photochem Photobiol 1996;64:182–7.
[31] Bigelow CE, Conover DL, Foster TH. Confocal fluorescence spectroscopy and anisotropy imaging system. Opt Lett 2003;28:695–7.
[32] Melnikova VO, Bezdetnaya LN, Bour C, Festor E, Gramain MP, Merlin JL, et al. Subcellular localisation of meta-tetra (hydroxyphenyl) chlorin in human tumor cells subjected to photodynamic treatment. J Photochem Photobiol B 1999;49:96–103.
[33] Matroule JY, Carthy CM, Granville DJ, Jolois O, Hunt DWC, Piette J. Mechanism of colon cancer cell apoptosis mediated by

pyropheophorbide-a methylester photosensitization. Oncogene 2001; 20:4070–84.

[34] Bernardi P, Scorrano L, Colonna R, Petronilli V, Di Lisa F. Mitochondria and cell death. Mechanistic aspects and methodological issues. Eur J Biochem 1999;264:687–701.

[35] Teiten MH, Marchal S, D'Hallewin MA, Guillemin F, Bezdetnaya L. Primary photodamage sites and mitochondrial events after Foscan photosnsitization of MCF-7 human breast cancer cells. Photochem Photobiol 2003;78:9–14.

[36] Morgan J, Oseroff AR. Mitochondria-based photodynamic anti-cancer therapy. Adv Drug Deliver Rev 2001;49:71–86.

[37] Chiu S-M, Xue L-Y, Usuda J, Azizuddin K, Oleinick NL. Bax is essential for mitochondrion-mediated apoptosis but not for cell death caused by photodynamic therapy. Br J Cancer 2003;89:1590–7.

[38] Vantieghem A, Xu Y, Declercq W, Vandenabeele P, Denecker G, Vandenheede JR, et al. Different pathways mediate cytochrome *c* release after photodynamic therapy with hypericin. Photochem Photobiol 2001;74:133–42.

[39] Reiners JJ, Caruso JA, Mathieu P, Chelladurai B, Yin XM, Kessel D. Release of cytochrome *c* and activation of pro-caspase-9 following lysosomal photodamage involves Bid cleavage. Cell Death Differ 2002;9:934–44.